

# Interleukin 6–Dependent Genomic Instability Heralds Accelerated Carcinogenesis Following Liver Regeneration on a Background of Chronic Hepatitis

Tali Lanton,<sup>1\*</sup> Anat Shriki,<sup>1\*</sup> Yael Nechemia-Arbely,<sup>1</sup> Rinat Abramovitch,<sup>1,2</sup> Orr Levkovitch,<sup>1</sup> Revital Adar,<sup>1</sup> Nofar Rosenberg,<sup>1</sup> Mor Paldor,<sup>1</sup> Daniel Goldenberg,<sup>1</sup> Amir Sonnenblick,<sup>3</sup> Amnon Peled,<sup>1</sup> Stefan Rose-John,<sup>4</sup> Eithan Galun,<sup>1</sup> and Jonathan H. Axelrod<sup>1</sup>

Liver cancer, which typically develops on a background of chronic liver inflammation, is now the second leading cause of cancer mortality worldwide. For patients with liver cancer, surgical resection is a principal treatment modality that offers a chance of prolonged survival. However, tumor recurrence after resection, the mechanisms of which remain obscure, markedly limits the long-term survival of these patients. We have shown that partial hepatectomy in multidrug resistance 2 knockout (*Mdr2*<sup>-/-</sup>) mice, a model of chronic inflammation-associated liver cancer, significantly accelerates hepatocarcinogenesis. Here, we explore the postsurgical mechanisms that drive accelerated hepatocarcinogenesis in *Mdr2*<sup>-/-</sup> mice by perioperative pharmacological inhibition of interleukin-6 (IL6), which is a crucial liver regeneration priming cytokine. We demonstrate that inhibition of IL6 signaling dramatically impedes tumorigenesis following partial hepatectomy without compromising survival or liver mass recovery. IL6 blockade significantly inhibited hepatocyte cell cycle progression while promoting a hypertrophic regenerative response, without increasing apoptosis. *Mdr2*<sup>-/-</sup> mice contain hepatocytes with a notable persistent DNA damage response ( $\gamma$ H2AX, 53BP1) due to chronic inflammation. We show that liver regeneration in this microenvironment leads to a striking increase in hepatocytes bearing micronuclei, a marker of genomic instability, which is suppressed by IL6 blockade. **Conclusion:** Our findings indicate that genomic instability derived during the IL6-mediated liver regenerative response within a milieu of chronic inflammation links partial hepatectomy to accelerated hepatocarcinogenesis; this suggests a new therapeutic approach through the usage of an anti-IL6 treatment to extend the tumor-free survival of patients undergoing surgical resection. (HEPATOLOGY 2017;65:1600-1611)

**A**ncedotal and experimental observations collected over the past century clearly indicate that surgical stress can dramatically accelerate the recurrence of cancers.<sup>(1)</sup> This is of particular relevance to patients with primary hepatic malignancies for which surgical resection, or partial hepatectomy (PH), is often the best option of treatment, in

particular for those patients who do not meet the Barcelona criteria for liver transplantation.<sup>(2,3)</sup>

Liver cancer is now the second leading cause of cancer mortality worldwide and currently presents a major health problem.<sup>(4)</sup> Hepatocellular carcinoma (HCC), the leading form of all primary liver cancers, typically appears following years of chronic hepatitis and is a

*Abbreviations:* Akt, AKT1; BrdU, 5-bromo-2'-deoxyuridine; CK19, cytokeratin 19; DAPI, 4,6-diamidino-2-phenylindole; HCC, hepatocellular carcinoma; IgG, immunoglobulin G; IL6, interleukin 6; mAb, monoclonal antibody; *Mdr2*, multidrug resistance 2; MRI, magnetic resonance imaging; PH, partial hepatectomy; MNi, micronuclei; STAT3, signal transducer and activator of transcription 3; WT, wild type.

Received July 12, 2016; accepted December 11, 2016.

Additional Supporting Information may be found at [onlinelibrary.wiley.com/doi/10.1002/hep.29004/supinfo](http://onlinelibrary.wiley.com/doi/10.1002/hep.29004/supinfo).

Y. Nechemia-Arbely's present address is: Ludwig Institute for Cancer Research and Department of Cellular and Molecular Medicine, University of California at San Diego, La Jolla, CA

devastating disease with a 5-year survival rate of only about 7%. But resection has dire ramifications as it is generally associated with poor survival, largely due to rates of tumor recurrence occurring within 5 years of treatment that can reach levels of 75%-80%.<sup>(2,3)</sup> Estimates indicate that undetected intrahepatic lesions contribute to 60%-70% of recurrences, while 30%-40% are due to *de novo* HCC lesions.<sup>(5)</sup>

While studies in animal models using transplanted tumor cells or chemical-induced tumors indicate that PH can significantly enhance most aspects of tumorigenesis, including initiation, promotion, growth, and metastasis,<sup>(6-10)</sup> the molecular and cellular mechanisms underlying this process remain largely undefined. Moreover, unlike these animal models, in most cases, human HCC is driven by chronic injury and inflammation of the liver due to chronic viral hepatitis, alcohol abuse, and/or nonalcoholic steatohepatitis.<sup>(11)</sup> Thus, currently, there is insufficient information about how liver regeneration affects hepatocarcinogenesis, particularly in an inflammatory microenvironment.

In previous studies, we and others have followed the development of liver fibrosis and determined the role of inflammation in the development of HCC in multidrug resistance 2 (*Mdr2*, *Abcb4*) knockout (*Mdr2*<sup>-/-</sup>) mice.<sup>(12-14)</sup> These mice lack the liver-specific P-glycoprotein, which causes regurgitation of toxic bile from leaky ducts and induces portal inflammation at an early

age (3 months), followed by dysplasia and slowly developing HCC (age 12-15 months). Adult human patients carrying mutations in the *MDR3/ABCB4* gene, the human ortholog of the murine *Mdr2* gene, also show an increased risk for dysplasia with later development of HCC and cholangiocarcinoma.<sup>(15)</sup> We recently modeled the human clinical condition of a patient undergoing PH by performing a similar procedure in chronically inflamed *Mdr2*<sup>-/-</sup> mice.<sup>(16)</sup> We showed that liver resection under high basal levels of cell cycle arrest, senescence, and apoptosis present in hepatocytes of *Mdr2*<sup>-/-</sup> mice strongly attenuates regeneration but dramatically accelerates hepatocarcinogenesis and tumor development.<sup>(16)</sup>

In the present study we examined the molecular and cellular mechanisms governing liver regeneration in order to gain insight into their roles in accelerated carcinogenesis. The process of liver regeneration is primed by cytokines, including interleukin-6 (IL6) secreted within hours following PH, and propagated by growth factors, including hepatic growth factor.<sup>(17)</sup> Interestingly, most observations indicate that IL6, although not a complete mitogen for hepatocytes *in vivo*, is critical to the early onset of the DNA synthetic response following PH and appears to mediate both promitotic and prosurvival activities.<sup>(18-22)</sup> We therefore set out to determine whether IL6 is also crucial for accelerated hepatocarcinogenesis.

\*These authors contributed equally to this study.

Supported by grants from the Israel Science Foundation (923/14, to J.H.A., and 692/12, to E.G.) and by the Israel Cancer Research Fund (J.H.A.); E.G. is also supported by grants from the Deutsche Forschungsgemeinschaft (SFB841 project C3), the DKFZ-MOST, the I-CORE ISF Center of Excellence (41/11), the MOST, the Jay Ruskin Foundation, the Robert H. Benson Trust, and the Selma Kron Foundation for student fellowships; S.R.J. is supported by grants from the Deutsche Forschungsgemeinschaft (SFB841 project C1) and by the Cluster of Excellence "Inflammation at Interfaces"; A.S. was supported by the Morasha program of the Israel Science Foundation (728/11) and the Israel Cancer Association (2014-0001).

Copyright © 2016 by the American Association for the Study of Liver Diseases.

View this article online at [wileyonlinelibrary.com](http://wileyonlinelibrary.com).

DOI 10.1002/hep.29004

Potential conflict of interest: Nothing to report.

## ARTICLE INFORMATION:

From the <sup>1</sup>Goldyne Savad Institute of Gene Therapy; <sup>2</sup>Magnetic Resonance Imaging/Magnetic Resonance Spectroscopy Laboratory, Human Biology Research Center, and <sup>3</sup>Sharett Institute of Oncology, Hadassah Medical Center, Jerusalem, Israel; <sup>4</sup>Institut für Biochemie, Christian-Albrechts-Universität zu Kiel, Kiel, Germany.

## ADDRESS CORRESPONDENCE AND REPRINT REQUESTS TO:

Jonathan H. Axelrod, Ph.D.  
Goldyne-Savad Institute of Gene Therapy  
Hadassah Hebrew University Hospital  
P.O. Box 12000

Jerusalem, 91120, Israel  
Tel: + 972-2-6778732  
E-mail: [axelrod@hadassah.org.il](mailto:axelrod@hadassah.org.il)

## Materials and Methods

### ANIMALS

Mdr2 *knockout* (Mdr2<sup>-/-</sup>) mice (FVB/NJ) (derived from FVB.129P2-Abcb4tm1Bor; The Jackson Laboratory) have been described.<sup>(16)</sup> Wild-type (WT) mice (FVB/NJ) were purchased from Harlan Laboratories Ltd. (Jerusalem, Israel). Mdr2<sup>-/-</sup> IL6<sup>-/-</sup> (C57BL/6) mice were derived by crossing Mdr2<sup>-/-</sup> (C57BL/6) mice<sup>(23)</sup> and IL6<sup>-/-</sup> (C57BL/6) mice (The Jackson Laboratory). Mice were maintained in an animal facility under specific pathogen-free conditions, at a temperature of ~23 °C in a 12-hour light-dark cycle, and received sterile commercial rodent chow and water *ad libitum*. Experimental procedures and animal maintenance were performed in accordance with Institutional Animal Care and Use Committee-approved animal treatment protocols (license no. OPRR-A01-5011). Two-thirds PH was performed as described<sup>(16,24)</sup> on 3-month-old and 6-month-old mice under ketamine and xylazine anesthesia in the morning and consisted of midline laparotomy with separate ligation and removal of the left and anterior median lobes. Antibody-mediated inhibition of IL6 was performed by injection of a rat neutralizing anti-IL6 immunoglobulin G1 (IgG<sub>1</sub>) monoclonal antibody (mAb; 100 µg, intravenously; MAB406; R&D Systems Inc.) or a rat IgG<sub>1</sub> isotype control mAb (100 µg, intravenously; MAB005; R&D Systems Inc.) reconstituted according to the manufacturer's instructions, diluted in normal saline, and administered immediately following PH. Mice were injected intraperitoneally with 5-bromo-2'-deoxyuridine (BrdU; Sigma-Aldrich, Rehovot, Israel) at 1 mg/mouse in 10 µL/1 g of body weight 3 hours prior to sacrifice by exsanguination while under ketamine and xylazine anesthesia. Upon sacrifice, livers were excised and weighed, and liver tumors with a diameter >2 mm were counted and measured. Liver specimens were either fixed in 4% buffered formalin or snap-frozen in liquid nitrogen for further analysis.

### MAGNETIC RESONANCE IMAGING ANALYSIS

*In vivo* assessment of tumor incidence was performed by magnetic resonance imaging (MRI) using a horizontal 4.7T BioSpec spectrometer (Bruker Corporation, Billerica, MA), using a bird cage coil. Mice were anesthetized (30 mg/kg of pentobarbital

intraperitoneally) and placed in a supine position, with the liver located at the center of the coil, as described.<sup>(16)</sup> Mice were scanned at 7, 8, 9, and 10 months of age; and liver hepatomegaly and tumor formation were evaluated from multislice coronal and axial T1-weighted and T2-weighted fast-spin echo images covering the entire liver, both coronally and axially (repetition time/echo time = 147/10 milliseconds; flip angle = 30 degrees; field of view = 5 cm; 256 × 256 pixels; 11-13 slices with slice thickness = 1 mm). Specimens were analyzed by an experienced operator in a blinded fashion.

### HISTOLOGY, IMMUNOHISTOCHEMISTRY, IMMUNOFLUORESCENCE, AND WESTERN BLOT ANALYSES

Livers samples were fixed in 4% buffered formaldehyde, followed by 80% ethanol and embedded in paraffin blocks. Sections (5 µm thick) were stained with hematoxylin and eosin by standard procedures. Immunohistochemistry and western blot analyses were performed using antibodies against BrdU (Dako, Denmark), Ki-67 (clone TEC-3, Dako), β-catenin (BD Biosciences, San Jose, CA), lamin B1 (Novus Biologicals, CO), phosphorylated signal transducer and activator of transcription 3 (STAT3), STAT3, (Santa Cruz Biotechnology, Santa Cruz, CA), phosphorylated AKT1 (AKT, Ser473) and AKT (Cell Signaling), anti-γH2AX (Millipore), anti-53BP1 (Bethyl Laboratories Inc.), anti-caspase-3 (Cell Signaling Technology Inc.), rabbit anti-cytokeratin 19 (CK19; Abcam), and β-actin antibody (Sigma). Immunostainings and western blots were developed with antimouse horseradish peroxidase polymer, anti-rabbit horseradish peroxidase polymer (Dako), or biotinylated rabbit antirat (for BrdU) and developed with 3-amino-9-ethylcarbazole. Immunofluorescent staining was visualized with Alexa Fluor 488 goat anti-mouse IgG (Life Technologies; for β-catenin, γH2AX), Alexa Fluor 635 goat antirabbit (Invitrogen; lamin, 53BP1), and donkey anti-rabbit(Cy3) (Jackson; CK19). For western blot analysis, protein extracts (50 µg) prepared from flash-frozen tissue samples (~100 mg) by homogenization were separated by polyacrylamide gel electrophoresis and subjected to western blot analysis as described.<sup>(24)</sup> Western blot bands were quantified using ImageJ Imaging software (National Institutes of Health).

## MEASUREMENT OF CELL SIZE

Digital images of liver thin sections (5  $\mu\text{m}$  thick) prepared from formalin-fixed, paraffin-embedded samples stained by immunofluorescence for  $\beta$ -catenin and 4,6-diamidino-2-phenylindole (DAPI) were photographed at a magnification of  $\times 40$ . Cell size of hepatocytes in zone 2 was measured as area in square pixels using ImageJ software in 100 hepatocytes/mouse by an observer who was blinded to the treatment groups.

## MICRONUCLEI ASSESSMENT

Micronuclei (MNi)-containing hepatocytes were assessed in paraffin-embedded thin sections by immunofluorescence staining for lamin and  $\beta$ -catenin and counterstained with DAPI. MNi were identified as lamin-coated, DAPI<sup>+</sup> bodies less than one quarter the size of the nucleus and visibly distinct from the nucleus and hepatocyte cell borders demarked by  $\beta$ -catenin, essentially as defined.<sup>(25)</sup> MNi-containing hepatocytes were quantified within photomicrographic images of immunofluorescently stained thin sections taken at an original magnification of  $\times 40$  and entailed scoring of about 400 hepatocytes/mouse by an observer who was blinded to the treatment groups.

## STATISTICAL ANALYSIS

Statistical comparisons using the indicated tests were performed using GraphPad Prism version 6.02 software (GraphPad Software), with  $P < 0.05$  considered statistically significant. Repeated measures analysis of variance was performed using SPSS Statistics Data Editor, version 22.

## Results

### IL6 BLOCKADE INHIBITS PH-INDUCED ACCELERATED CARCINOGENESIS

In order to determine the role of IL6 in accelerated hepatocarcinogenesis following liver regeneration, we initially subjected Mdr2<sup>-/-</sup> single-knockout (C57BL/6) and Mdr2-IL6 double-knockout (Mdr2<sup>-/-</sup>IL6<sup>-/-</sup>, C57BL/6) mice to PH. However, while about 90% (14/16) of the single-knockout Mdr2<sup>-/-</sup> mice survived long term, most (8/12) of the double-knockout mice perished within 6 months after surgery ( $P = 0.0054$  by Fisher's exact test), perhaps reflecting the sensitivity of

IL6 knockout mice to liver resection.<sup>(18,21,22)</sup> In contrast, we found that a single administration of an anti-IL6 mAb (100  $\mu\text{g}$ , intravenously) to Mdr2<sup>-/-</sup> (FVB/NJ) mice, the strain used in our previous study,<sup>(16)</sup> at the time of resection did not diminish survival of the resected mice. Following perioperative administration of IL6 mAb at this dose, circulating IL6 protein in the Mdr2<sup>-/-</sup> mice became undetectable at 9 hours post-PH (Supporting Fig. S1).

Therefore, to examine whether IL6 supports accelerated hepatocarcinogenesis following liver regeneration, we subjected Mdr2<sup>-/-</sup> (FVB/NJ) mice to PH at 3 months of age and treated the mice at the time of surgery with either the IL6 mAb in order to temporarily inhibit IL6 activity or a control IgG mAb (Supporting Fig. S2). We then monitored the resected mice for tumor development by MRI analysis at 7, 8, 9, and 10 months of age and by visual scoring upon sacrifice at the age of 10 months (Supporting Fig. S2). MRI analysis revealed that IL6 blockade strongly delayed the appearance of liver tumors in the resected mice, leading to a striking 3-fold reduction in tumor incidence in comparison to control mAb-treated mice (Fig. 1A,D). Additional analysis by visual scoring confirmed the observations of the MRI analysis and further showed that IL6 mAb treatment dramatically reduced tumor load but reduced tumor volume only marginally and without statistical significance (Fig. 1C-F, solid bars and symbols).

These observations suggested that IL6 expression following PH may function to drive tumor initiation or perhaps to promote progression of cancerous or precancerous cells. We therefore reasoned that if liver regeneration promotes tumor progression, then allowing more time for precancerous cells or microtumors to accumulate in the liver prior to resection might be expected to increase tumorigenesis. To test this hypothesis, we subjected Mdr2<sup>-/-</sup> mice to PH at the age of 6 months together with treatment with either IL6 mAb or control IgG at the time of surgery. Analysis for tumor development by visual scoring upon sacrifice at 10 months of age demonstrated that IL6 blockade following PH performed at 6 months of age also dramatically reduced both tumor incidence and tumor load (Fig. 1D,E). However, a comparison of tumors appearing in the control IgG-treated mice following PH showed slight decreases in tumor load and in tumor volume in mice resected at 6 months of age compared to mice resected at 3 months, without statistical significance ( $P = 0.65$  and  $P = 0.12$ , respectively, by two-tailed Mann-Whitney test) (Fig. 1E,F, solid versus open symbols). Also, no differences in tumorigenesis were observed in the IL6

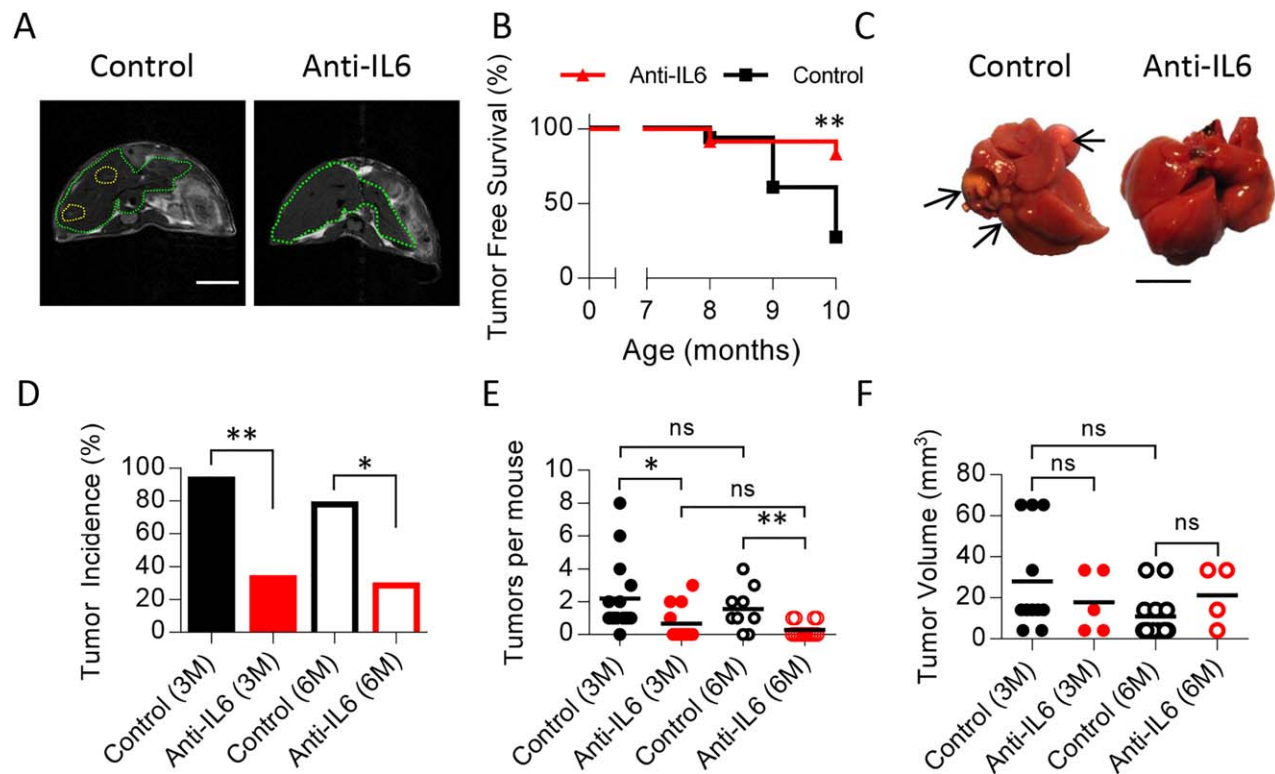


**FIG. 1.** IL6 blockade following PH reduces tumorigenesis in  $Mdr2^{-/-}$  mice. (A) Representative serial MRIs of individual mice aged 10 months that were subjected to two-thirds PH at 3 months of age and immediately treated with either anti-IL6 mAb or control IgG mAb. Green hatched lines denote the liver contours, and yellow hatched lines denote tumor masses. Scale bar, 1 cm. (B) Kaplan-Meir plot of liver tumor-free survival as determined by MRI analysis in  $Mdr2^{-/-}$  mice in (A).  $**P < 0.01$  using log rank test,  $n = 12-15$ . (C) Photographs of representative livers removed from mice 7 months after PH performed at the age of 3 months. Arrows indicate tumors. Scale bars, 1 cm. (D) Tumor incidence assessed by visual scoring upon sacrifice at 10 months of age in  $Mdr2^{-/-}$  mice subjected to PH at 3 or 6 months of age and treated with either anti-IL6 or control mAb were analyzed using two-tailed Fischer's exact test.  $*P < 0.05$ ,  $**P < 0.01$ . (E) Tumor load per mouse liver and (F) tumor volume at 10 months of age. Data of individual mice (E) and tumors (F) were means-analyzed using a two-tailed Mann-Whitney test.  $*P < 0.05$ ,  $**P < 0.01$ ; anti-IL6,  $n = 12$  and  $n = 14$ ; control IgG,  $n = 15$  and  $n = 9$  for PH at 3 and 6 months, respectively. Abbreviation: ns, nonsignificant.

mAb-treated mice resected at 3 and 6 months of age. This finding is consistent with the notion that events proximal to PH, but not those accumulating in time prior to PH, determined the tumorigenic outcome. Because CK19 expression has been reported to predict early post-operative recurrence and aggressiveness in some human HCCs,<sup>(26)</sup> we examined CK19 expression in  $Mdr2^{-/-}$  mice with or without IL6 mAb treatment. However this analysis revealed that IL6 mAb treatment did not affect the levels of CK19 expression in the tumors and dysplastic nodules, which were largely negative for CK19 staining (Supporting Fig. S3). Importantly, the effect of IL6 blockade was evident only within the context of the regenerative response as administration of the IL6 and control mAbs at 3 months of age without PH had no apparent effect on tumor incidence at 10 months of age (9/9 for anti-IL6 versus 8/10 for control mAb-treated

mice, respectively,  $P = 0.47$  by Fischer's exact test). Thus, IL6 blockade markedly reduced tumorigenesis and improved tumor-free survival in mice with chronic inflammation that undergo liver resection.

## IL6 BLOCKADE INDUCES A HYPERPLASTIC TO HYPERTROPHIC SWITCH FOLLOWING PH

In order to uncover the cellular mechanisms through which IL6 supports accelerated carcinogenesis in the context of chronic hepatitis, we next examined the role of IL6 in liver regeneration in the  $Mdr2^{-/-}$  mice.

Liver regeneration normally begins with a priming phase mediated by IL6 and tumor necrosis factor  $\alpha$ ,

which is followed by a burst of regenerative activity during which most of the hepatocytes enter the cell cycle.<sup>(17)</sup> We have shown that liver regeneration is strongly attenuated in *Mdr2*<sup>-/-</sup> mice, as manifested by a blunted DNA synthetic response and the accumulation of hepatocytes arrested within the cell cycle.<sup>(16)</sup> However, during regeneration, IL6 is also crucial for the protection from necrosis and apoptosis,<sup>(18,20,22)</sup> which, in principle, can also function to restrict tumorigenesis. Indeed, nuclear factor  $\kappa$ B-mediated protection from apoptosis has been identified as an important mechanism in promoting tumorigenesis in *Mdr2*<sup>-/-</sup> mice.<sup>(13)</sup>

We therefore examined the effect of IL6 blockade by mAb inhibition on hepatocyte apoptosis and the regenerative response following PH. Surprisingly, analyses of apoptosis by caspase-3 immunostaining (Fig. 2A) and by terminal deoxynucleotidyl transferase-mediated deoxyuridine triphosphate nick-end labeling (data not shown) showed that apoptosis levels did not increase following PH and were not affected by the IL6 mAb treatment. On the other hand, analysis of mitotic response in hepatocytes following PH by immunostaining for Ki-67 and BrdU uptake demonstrated a small but significant 2-fold increase in the number of hepatocytes entering the cell cycle 48 hours post-PH (Fig. 2B,C). Notably, perioperative inhibition of IL6 reduced the mitotic response in *Mdr2*<sup>-/-</sup> mice by between 70% and 50%, as indicated by Ki67 ( $P < 0.01$ ) and BrdU<sup>+</sup> ( $P = 0.057$ ) immunostaining, respectively (Fig. 2B,C), and had a similar effect in WT mice (Supporting Fig. S4). Curiously, despite the low hepatocyte proliferative response, IL6 mAb-treated mice displayed no impairment in the recovery of liver mass in comparison to control-treated mice during the week following PH or at the age of 10 months (Supporting Fig. S5). This suggests that an alternative mechanism drives liver regeneration following PH in *Mdr2*<sup>-/-</sup> mice subjected to IL6 blockade.

Recovery of liver mass following resection is governed by both hyperplastic and hypertrophic responses, controlled, respectively, by the STAT3 and by AKT/mammalian target of rapamycin complex 1 signaling pathways.<sup>(27-29)</sup> In the absence of STAT3 activation, recovery of liver mass can occur through AKT/mammalian target of rapamycin complex 1-mediated hypertrophy of the hepatocytes.<sup>(28,29)</sup> Western blot analysis of liver samples taken shortly following PH showed that STAT3 phosphorylation, which is largely IL6-mediated during liver regeneration,<sup>(18)</sup> increased in the *Mdr2*<sup>-/-</sup> mice 24 hours post-PH and, as expected, was significantly diminished by IL6 blockade (Fig. 3A). In contrast, levels of

phosphorylated AKT, which were not substantially elevated in control-treated mice at either time point, increased by about 10-fold at 48 hours post-PH in IL6 mAb-treated mice (Fig. 3A). We therefore postulated that restoration of liver size in the IL6 mAb-treated mice was a function of growth in cell size rather than cell proliferation. Analysis of hepatocyte cell size showed that, while cell size did not change 4 days post-PH, by 6 days following PH hepatocytes in IL6 mAb-treated mice were significantly larger than both the hepatocytes prior to PH and those in the mice treated with control mAb (Fig. 3B,C). Indeed, the hepatocytes of IL6 mAb-treated mice increased in size by about 36% to  $1,329 \pm 53$  pixels (mean  $\pm$  standard error of the mean) in comparison to their size prior to surgery ( $977 \pm 38$  pixels), whereas the hepatocytes of the control-treated mice increased in size by only one half as much, i.e.,  $\sim 17\%$  ( $1,148 \pm 48$  pixels) (Fig. 3D). Curiously, increased hepatocyte cell size following IL6 inhibition was not observed in WT mice following PH (data not shown). As expected, the percentage of polynucleated hepatocytes in *Mdr2*<sup>-/-</sup> mice was significantly reduced following PH,<sup>(30,31)</sup> suggesting a reduction in polyploidy<sup>(32)</sup>; but their levels returned to baseline by the age of 10 months and were not affected by IL6 inhibition at either stage (Supporting Fig. S6). Taken together, these findings suggest that accelerated hepatocarcinogenesis is closely linked to cell cycle progression rather than protection from apoptosis and that in the absence of IL6, a hypertrophic regenerative response compensates for the reduced hyperplastic response following PH in *Mdr2*<sup>-/-</sup> mice.

## GENOMIC INSTABILITY IS INCREASED BY PH AND PREVENTED BY IL6 BLOCKADE

During early liver inflammatory stages, hepatocytes of *Mdr2*<sup>-/-</sup> mice possess pronounced genomic instability.<sup>(16)</sup> This is manifested by an elevated chromosomal instability gene expression signature and also by the presence of double-stranded DNA breaks, revealed by the activation of DNA damage response pathways and the presence of coimmunofluorescence stained foci of phosphorylated  $\gamma$ H2AX and 53BP1 (Supporting Fig. S7).<sup>(16)</sup> Because replicative stress and the presence of double-stranded breaks during cell division can give rise to genomic instability,<sup>(33)</sup> we postulated that the hyperplasia during liver regeneration may lead to enhanced genomic instability in *Mdr2*<sup>-/-</sup> mice and underlie the acceleration of carcinogenesis.<sup>(16)</sup> MNi and other nuclear anomalies are generated from

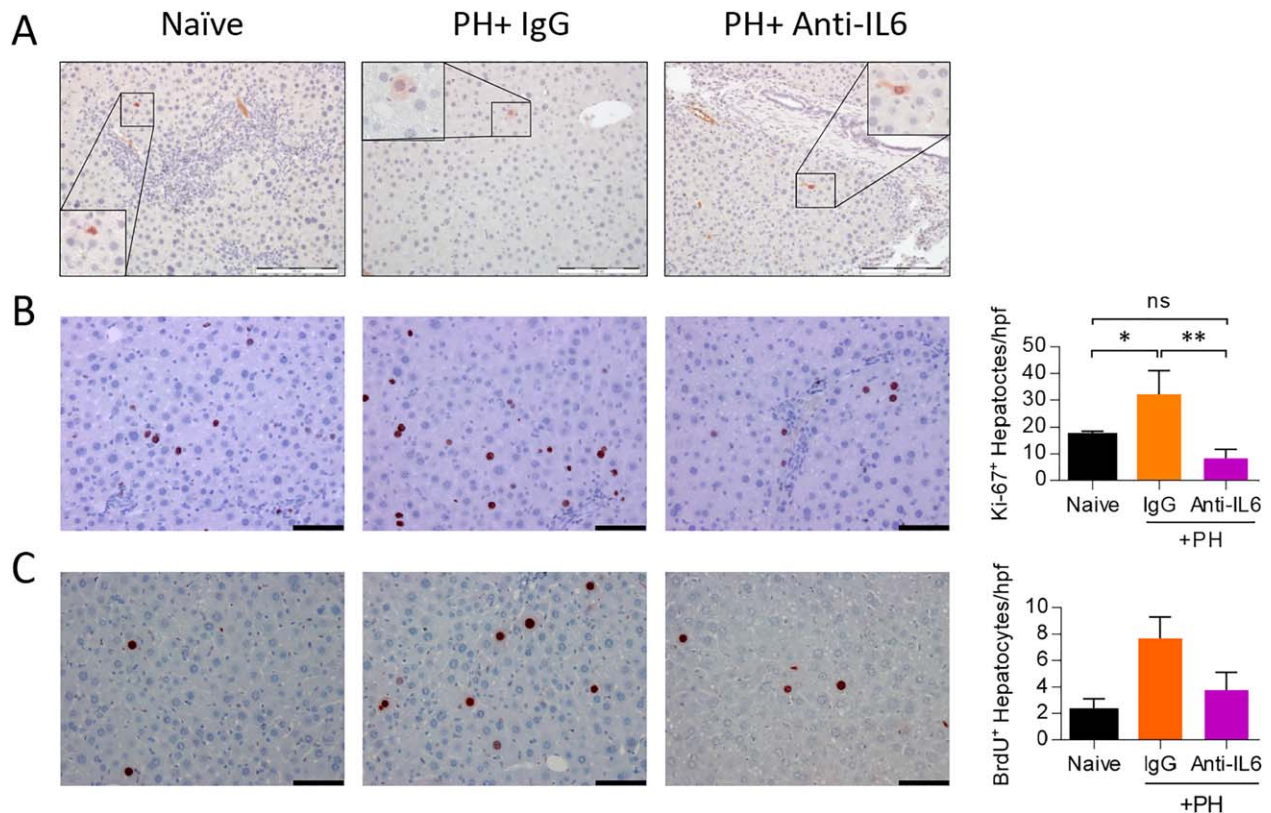


**FIG. 2.** IL6 blockade following PH inhibits the hepatocyte mitotic response but not apoptosis in *Mdr2*<sup>-/-</sup> mice. (A) Representative photomicrographs of cleaved caspase-3 immunostaining (red staining) in thin sections of livers taken 48 hours post-PH in *Mdr2*<sup>-/-</sup> mice aged 3 months and treated with either anti-IL6 mAb or control mAb (IgG) at the time of resection. Original magnification  $\times 20$  (inset  $\times 40$ ). Scale bars, 100  $\mu\text{m}$ . (B,C) Representative photomicrographs of Ki67 (B) and BrdU (C) immunostaining (red nuclear staining) in livers from (A) and quantification (right). Data are mean  $\pm$  standard error of the mean, \* $P < 0.05$ , \*\* $P < 0.01$  by one-tailed Mann-Whitney test, (B) (naive  $n = 18$ , anti-IL6  $n = 6$ , IgG  $n = 8$ ), and (C) (naive  $n = 3$ , anti-IL6  $n = 4$ , IgG  $n = 4$ ). Abbreviations: hpf, hours postfertilization; ns, nonsignificant.

lagging chromosomes during defective cell division.<sup>(34-37)</sup> Because they are strongly correlated with mitotic errors, MNi are regarded as an accurate indicator of genomic instability and as biomarkers of genotoxic events related to mutagen exposure.<sup>(34-37)</sup> In order to assess the effect of PH on genomic instability in mice with chronic hepatitis, we compared levels of MNi in hepatocytes before and following PH in *Mdr2*<sup>-/-</sup> and WT mice.

Using immunofluorescence staining, which accurately identifies MNi according to their characteristic features as small, lamin-coated, extranuclear DNA bodies,<sup>(25)</sup> we quantified the micronucleated (MNi<sup>+</sup>) hepatocytes before PH and on days 2 and 6 following PH in WT and *Mdr2*<sup>-/-</sup> mice treated with either control or IL6 mAbs at the time of resection. This analysis clearly identified the presence of MNi in the hepatocytes of *Mdr2*<sup>-/-</sup> mice (Fig. 4A; Supporting Fig. S81),

most of which appeared to be encased within lamin-coated nuclear envelopes. MNi appeared to be present in about  $0.17 \pm 0.04\%$  (mean  $\pm$  standard error of the mean) of the hepatocytes in naive WT mice (Fig. 4B). In contrast, in *Mdr2*<sup>-/-</sup> mice, MNi<sup>+</sup> hepatocytes appeared to be significantly more widespread, representing  $0.46 \pm 0.06\%$  ( $P = 0.001$ , by Mann-Whitney test) of total hepatocytes before PH. Interestingly, we observed that MNi in *Mdr2*<sup>-/-</sup> hepatocytes occasionally stained positive for BrdU or Ki-67 by immunostaining, independent of that in the nucleus (Supporting Figs. S9 and S10), suggesting that MNi in *Mdr2*<sup>-/-</sup> mice may undergo asynchronous DNA replication relative to the primary nucleus.<sup>(38)</sup> Following PH, the levels of MNi<sup>+</sup> hepatocytes in the *Mdr2*<sup>-/-</sup> mice remained relatively unchanged for about 2 days in both experimental and control mice but then dramatically

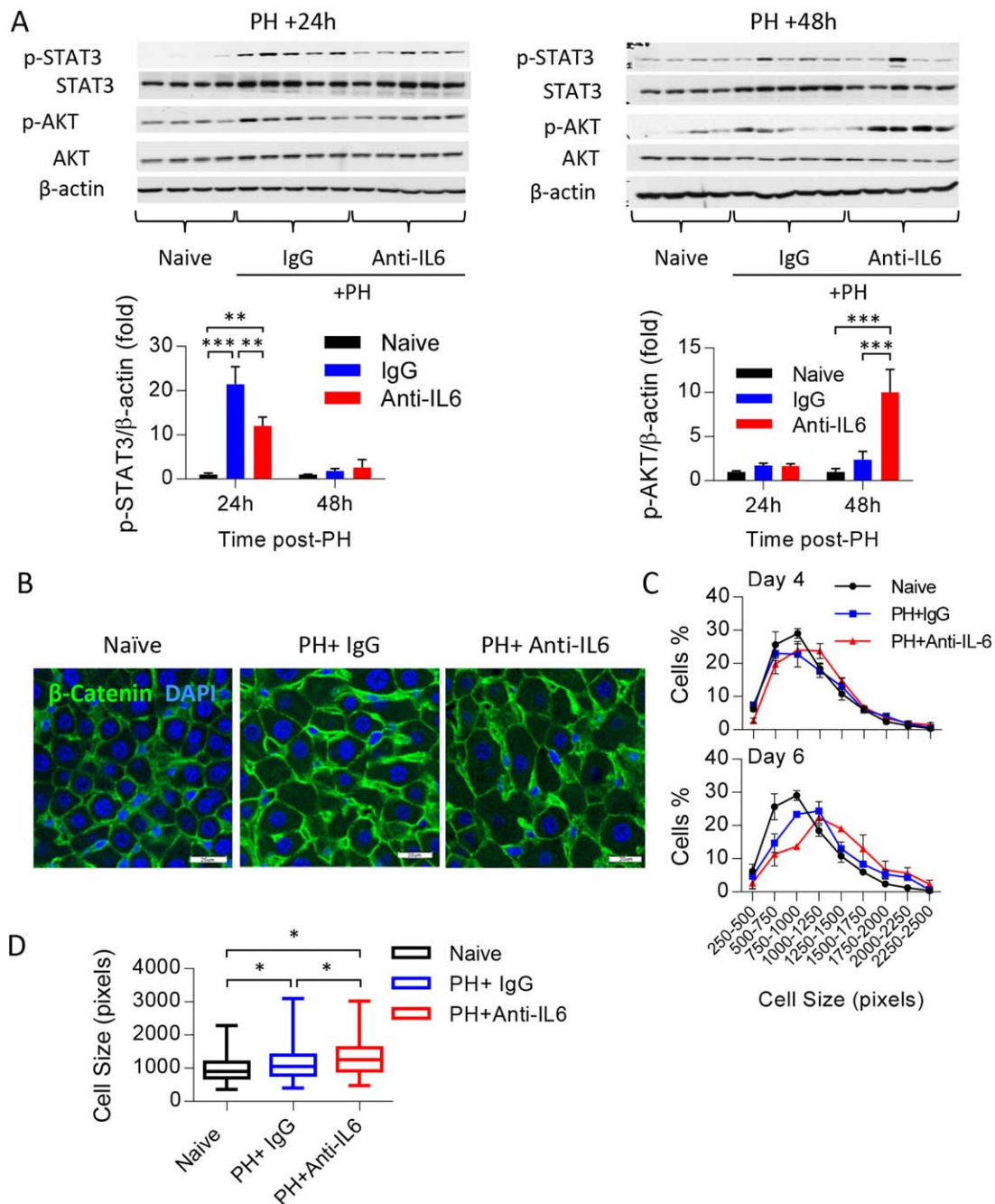


**FIG. 3.** IL6 blockade generates a hyperplastic to hypertrophic switch in the regenerative response following PH in *Mdr2*<sup>-/-</sup> mice. (A) Western blot analysis and quantification (below) of phosphorylated STAT3 (pSTAT3) and phosphorylated AKT (pAKT) in livers from naive mice and mice 24 and 48 hours post-PH and treated with either anti-IL6 mAb or control mAb (IgG). Data are means  $\pm$  standard error of the mean as fold change versus naive of the same blot. \* $P < 0.05$ , \*\* $P < 0.01$ , \*\*\* $P < 0.001$  by two-way analysis of variance ( $n = 5$ ). (B) Representative microphotographs of  $\beta$ -catenin (green) immunofluorescence staining of liver sections from mice before and 6 days post-PH with control IgG or anti-IL6 treatment. Sections are counterstained with DAPI to show nuclei (blue). Scale bars, 20  $\mu$ m. (C) Cell size distribution before and 4 days (above) and 6 days (below) after surgery in hepatectomized livers of naive (black), IL6 mAb-treated (red), and control mAb-treated (blue) *Mdr2*<sup>-/-</sup> mice. Each data point is representative of at least three mice.  $P = 0.002$  for the pattern of change between groups on day 6 post-PH by repeated measures analysis of variance. (D) Quantification of hepatocyte cell size in livers shown in (C). \* $P < 0.05$  by one-tailed Mann-Whitney test ( $n = 3-5$ ).

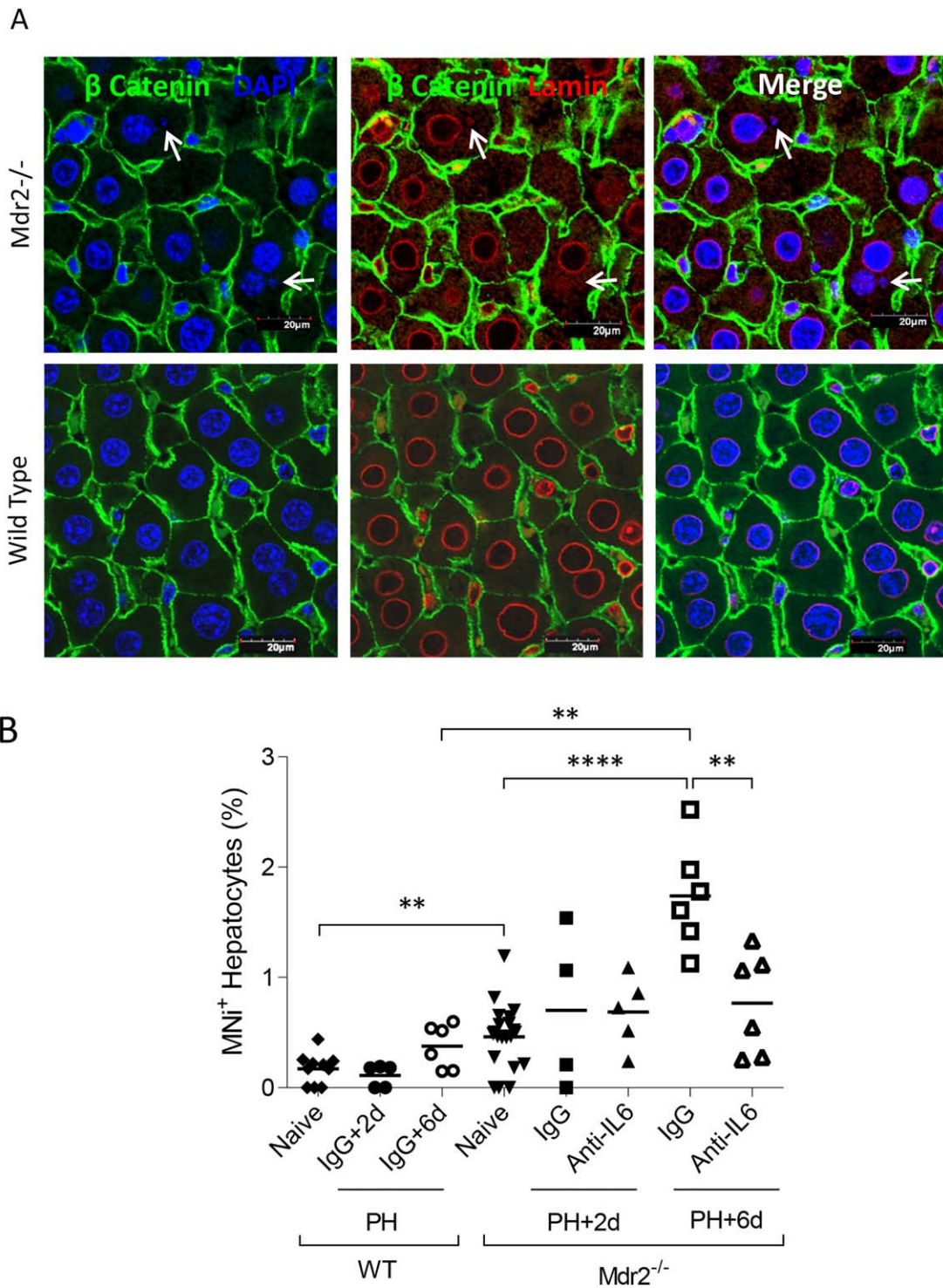


**FIG. 4.** PH generates micronuclei in hepatocytes of  $Mdr2^{-/-}$  mice and is prevented by IL6 blockade. (A) Representative confocal microscopic photomicrographs of immunofluorescently stained liver sections from naive  $Mdr2^{-/-}$  and WT mice, double-stained for lamin (red) and  $\beta$ -catenin (green) and counterstained with DAPI to show DNA (blue) in nuclei and MNi (arrows). Scale bars, 20  $\mu$ m. (B) Quantification of MNi<sup>+</sup> hepatocytes in immunofluorescently stained livers of WT and  $Mdr2^{-/-}$  mice before PH and 2 and 6 days following PH in mice treated with control IgG or anti-IL6 mAbs. Data are means (bar) and individual mice (symbols). \*\* $P < 0.01$  and \*\*\*\* $P < 0.0001$  using two-tailed Mann-Whitney test ( $n = 4-21$ ).

increased 4-fold to  $1.74 \pm 0.20\%$  ( $P < 0.0001$ ) by day 6 post-PH in the control IgG-treated mice. However, treatment with IL6 mAb reduced the levels of MNi<sup>+</sup> hepatocytes by more than 2-fold. In WT mice, the levels of MNi<sup>+</sup> hepatocytes did not change significantly following PH in comparison to naive controls ( $P = 0.126$ , by Mann-Whitney test), in agreement with previous reports.<sup>(39,40)</sup> These observations indicate that the high baseline levels of genomic instability in the hepatocytes of Mdr2<sup>-/-</sup> mice strikingly increase following liver resection but are prevented by IL6 blockade, in close correlation with its effect on accelerated hepatocarcinogenesis.

## Discussion

The risk of initiation of secondary hepatic cancers following surgical procedures remains an enormous therapeutic challenge to the long-term cancer-free survival of liver cancer patients. Our findings demonstrate that IL6, as an integral element of the cytokine signaling pathways driving liver regeneration,<sup>(17,18)</sup> is also crucial to the process of accelerated hepatocarcinogenesis following liver resection. Inhibition of IL6 during liver regeneration reduced STAT3 phosphorylation, while leading to strong AKT activation followed by a diversion from a hyperplastic regenerative response to a hypertrophic response and subsequently reduced carcinogenesis. These observations are supported by previous reports that STAT3 and AKT govern the alternative pathways of liver regeneration<sup>(27-29,41)</sup> and by the direct linkage between STAT3 and cancer observed previously.<sup>(42)</sup> Although AKT is also frequently hyperactivated in human cancers and is targeted for cancer therapy, our observation that AKT activation is associated with a reduction in cancer is supported by recent data showing that combined deletion of AKT isoforms leads to spontaneous liver cancer in mice.<sup>(43)</sup>

But how does IL-6 accelerate hepatocarcinogenesis? Our findings identify genomic instability enhanced during liver regeneration as a probable underlying mechanism that links surgical resection to accelerated hepatocarcinogenesis within a milieu of chronic inflammation. Interestingly, while our previous study showed that PH promotes tumor progression in terms of growth and number,<sup>(16)</sup> the findings of the present study indicate that perioperative inhibition of IL6 primarily affects tumor incidence and tumor load, a reflection of tumor-initiating events.

As shown in our previous studies<sup>(16)</sup> and confirmed here, the environment of bile-induced oxidative stress,

chronic liver injury, and chronic inflammation in Mdr2<sup>-/-</sup> mice gives rise to a persistent DNA damage response in hepatocytes. In this genotoxic environment, it is conceivable that physiological pressure to maintain metabolic homeostasis in the face of tissue loss imposes an IL6-initiated regenerative regime on hepatocytes, including those harboring DNA damage, leading to defective cell division, MNi formation, increased mutagenesis and genomic instability, and accelerated liver cancer. Severe genotoxicity can also lead to apoptosis, which can act to limit liver cancer.<sup>(13)</sup> But this apparently was not the case here as a role for IL6 in the context of hepatocyte protection from apoptosis in the resected Mdr2<sup>-/-</sup> was not observed.

In this study, we assessed MNi in order to quantify genomic instability in Mdr2<sup>-/-</sup> mice. MNi and other nuclear anomalies are well-established biomarkers of genotoxic events and chromosomal instability and are commonly associated with cancer and precarcinogenic states.<sup>(34-37)</sup> MNi also reportedly feature in hepatocytes of human patients with chronic hepatitis and appear to progressively increase in number from cirrhotic nodules to large regenerative nodules to dysplastic nodules and HCC.<sup>(44)</sup> However, we report a direct linkage of MNi to tumor promotion following surgical resection in a chronically inflamed liver.

Here, we show that MNi, which are inherently elevated in hepatocytes of Mdr2<sup>-/-</sup> mice, increase in an IL6-dependent fashion during liver regeneration together with the acceleration of tumorigenesis. This strongly supports the notion that MNi may be integral to the mutagenic events promoting carcinogenesis in an inflamed liver. Studies in cultured cells have identified functional defects in DNA replication and DNA-damage repair in MNi, which serve as a source of chromosome pulverization.<sup>(38)</sup> Our observation that some MNi may be undergoing asynchronous DNA replication relative to the primary nucleus (Supporting Figs. S7 and S8) suggests that perhaps these MNi similarly serve as a source of pulverized chromosomes in Mdr2<sup>-/-</sup> hepatocytes. Moreover, recent evidence from Stephens et al.<sup>(45)</sup> and from Zhang et al.<sup>(46)</sup> points to MNi as a source of a unique form of genetic instability and mutation in cancer cells, called *chromothripsis*, in which a single catastrophic event gives rise to tens to hundreds of chromosomal rearrangements localized to a limited number of genomic regions in the nucleus. This raises the intriguing possibility that the MNi produced by or reincorporated into the nucleus during liver regeneration may contribute to accelerated hepatocarcinogenesis through a mechanism involving

chromothripsis. Thus, it is possible that the genomic changes that involve gene amplifications unique to tumors from mice subjected to PH, but not in the spontaneous tumors from sham-treated mice, as we have reported,<sup>(16)</sup> may in part be the product of chromothripsis-like events involving MNI.

It is striking to note that the increase in micronucleated hepatocytes following PH in *Mdr2*<sup>-/-</sup> mice is similar in magnitude to that reported by others following PH in mice to which various chemical carcinogens were administered, including the genotoxin diethylnitrosamine, which is also a strong hepatotoxin.<sup>(39,40)</sup> This implies that, in terms of its potential to induce genomic instability, chronic injury and inflammation when coupled with regenerative stress in the liver appear to promote genomic instability not unlike that of strong chemical carcinogens. Moreover, IL6 has been shown to be crucial for diethylnitrosamine-induced HCC, particularly in male, obese mice, although the mechanism by which IL6 promotes HCC remains unclear.<sup>(47,48)</sup> Because both diethylnitrosamine treatment and liver resection involve the acute loss of tissue mass, it is tempting to postulate that in these and similar circumstances the regenerative role of IL6, with its apparent propensity to support genomic instability, defines its protumorigenic character. Nevertheless, the question of whether chronic IL6 expression also supports hepatocarcinogenesis on a background of chronic hepatitis in the absence of liver regeneration remains to be answered.

As surgery remains a principal potential treatment for patients with liver cancer, we sought to elucidate the mechanisms of surgery-enhanced tumor recurrence in order to ultimately improve long-term outcomes. Our findings indicate that the perioperative period is a key window of opportunity to counter the protumorigenic ramifications of surgery-induced liver regeneration. Our observation that pharmaceutical inhibition of IL6 prevents the accelerated emergence of liver cancer without increased mortality suggests a new and simple therapeutic approach to extend the tumor-free survival of liver cancer patients following surgical resection. In this respect, it is of interest to note that several inhibitors of IL6 signaling are currently approved or in development for clinical use.<sup>(49)</sup> The findings of this study provide preliminary evidence that support perioperative administration of IL6 inhibitors as a means to reduce the risk of tumor recurrence in liver cancer patients undergoing resection and provide the rationale for their potential evaluation in future clinical trials. However, new therapeutic strategies that prevent tumor recurrence after surgery need to be explored. In this regard, the aim of enhancing the hypertrophic over the

hyperplastic regenerative response may serve as a useful guide to uncover novel strategies and compounds that prevent the initiation of secondary cancers following surgical stress in patients with chronic hepatitis.

*Acknowledgment:* The authors are grateful to Deborah Olam for technical assistance; to Neta Barashi, Kobi (Jacob) Rachmilewitz, and Sharona Evan-Ram for helpful discussions and invaluable advice; and to Mindy M. Schimmel and Tali Bdolah-Abram for expert advice on statistical evaluation.

## REFERENCES

- 1) Demicheli R, Retsky MW, Hrushesky WJ, Baum M, Gukas ID. The effects of surgery on tumor growth: a century of investigations. *Ann Oncol* 2008;19:1821-1828.
- 2) Llovet JM. Updated treatment approach to hepatocellular carcinoma. *J Gastroenterol* 2005;40:225-235.
- 3) Schwartz M, Roayaie S, Konstadoulakis M. Strategies for the management of hepatocellular carcinoma. *Nat Clin Pract Oncol* 2007;4:424-432.
- 4) Torrecilla S, Llovet JM. New molecular therapies for hepatocellular carcinoma. *Clin Res Hepatol Gastroenterol* 2015;39(Suppl. 1):S80-S85.
- 5) Llovet JM, Schwartz M, Mazzaferro V. Resection and liver transplantation for hepatocellular carcinoma. *Semin Liver Dis* 2005;25:181-200.
- 6) Solt DB, Cayama E, Tsuda H, Enomoto K, Lee G, Farber E. Promotion of liver cancer development by brief exposure to dietary 2-acetylaminofluorene plus partial hepatectomy or carbon tetrachloride. *Cancer Res* 1983;43:188-191.
- 7) Rizvi TA, Mathur M, Nayak NC. Enhancement of aflatoxin B1-induced hepatocarcinogenesis in rats by partial hepatectomy. *Virchows Arch B Cell Pathol Incl Mol Pathol* 1989;56:345-350.
- 8) Hanigan MH, Winkler ML, Drinkwater NR. Partial hepatectomy is a promoter of hepatocarcinogenesis in C57BL/6J male mice but not in C3H/HeJ male mice. *Carcinogenesis* 1990;11:589-594.
- 9) Loizidou MC, Lawrance RJ, Holt S, Carty NJ, Cooper AJ, Alexander P, et al. Facilitation by partial hepatectomy of tumor growth within the rat liver following intraportal injection of syngenic tumor cells. *Clin Exp Metastasis* 1991;9:335-349.
- 10) de Jong KP, Lont HE, Bijma AM, Brouwers MA, de Vries EG, van Veen ML, et al. The effect of partial hepatectomy on tumor growth in rats: *in vivo* and *in vitro* studies. *HEPATOLOGY* 1995; 22:1263-1272.
- 11) Llovet JM, Zucman-Rossi J, Pikarsky E, Sangro B, Schwartz M, Sherman M, et al. Hepatocellular carcinoma. *Nat Rev Dis Primers* 2016;2:16018.
- 12) Mauad TH, van Nieuwkerk CM, Dingemans KP, Smit JJ, Schinkel AH, Notenboom RG, et al. Mice with homozygous disruption of the *mdr2* P-glycoprotein gene. A novel animal model for studies of nonsuppurative inflammatory cholangitis and hepatocarcinogenesis. *Am J Pathol* 1994;145:1237-1245.
- 13) Pikarsky E, Porat RM, Stein I, Abramovitch R, Amit S, Kasem S, et al. NF-kappaB functions as a tumour promoter in inflammation-associated cancer. *Nature* 2004;431:461-466.

- 14) Fickert P, Fuchsichler A, Wagner M, Zollner G, Kaser A, Tilg H, et al. Regurgitation of bile acids from leaky bile ducts causes sclerosing cholangitis in Mdr2 (Abcb4) knockout mice. *Gastroenterology* 2004;127:261-274.
- 15) Wendum D, Barbu V, Rosmorduc O, Arrive L, Flejou JF, Poupon R. Aspects of liver pathology in adult patients with MDR3/ABCB4 gene mutations. *Virchows Arch* 2012;460:291-298.
- 16) Barash H, Gross RE, Edrei Y, Ella E, Israel A, Cohen I, et al. Accelerated carcinogenesis following liver regeneration is associated with chronic inflammation-induced double-strand DNA breaks. *Proc Natl Acad Sci USA* 2010;107:2207-2212.
- 17) Fausto N, Campbell JS, Riehle KJ. Liver regeneration. *HEPATOLOGY* 2006;43(Suppl. 1):S45-S53.
- 18) Cressman DE, Greenbaum LE, DeAngelis RA, Ciliberto G, Furth EE, Poli V, et al. Liver failure and defective hepatocyte regeneration in interleukin-6-deficient mice. *Science* 1996;274:1379-1383.
- 19) Sakamoto T, Liu Z, Murase N, Ezure T, Yokomuro S, Poli V, et al. Mitosis and apoptosis in the liver of interleukin-6-deficient mice after partial hepatectomy. *HEPATOLOGY* 1999;29:403-411.
- 20) Kovalovich K, DeAngelis RA, Li W, Furth EE, Ciliberto G, Taub R. Increased toxin-induced liver injury and fibrosis in interleukin-6-deficient mice. *HEPATOLOGY* 2000;31:149-159.
- 21) Blindenbacher A, Wang X, Langer I, Savino R, Terracciano L, Heim MH. Interleukin 6 is important for survival after partial hepatectomy in mice. *HEPATOLOGY* 2003;38:674-682.
- 22) **Wuestefeld T, Klein C, Streetz KL, Betz U, Lauber J, Buer J, et al.** Interleukin-6/glycoprotein 130-dependent pathways are protective during liver regeneration. *J Biol Chem* 2003;278:11281-11288.
- 23) Barashi N, Weiss ID, Wald O, Wald H, Beider K, Abraham M, et al. Inflammation-induced hepatocellular carcinoma is dependent on CCR5 in mice. *HEPATOLOGY* 2013;58:1021-1030.
- 24) Nechemia-Arbely Y, Shriki A, Denz U, Drucker C, Scheller J, Raub J, et al. Early hepatocyte DNA synthetic response posthepatectomy is modulated by IL-6 trans-signaling and PI3K/AKT activation. *J Hepatol* 2011;54:922-929.
- 25) Igarashi M, Shimada H. An improved method for the mouse liver micronucleus test. *Mutat Res* 1997;391:49-55.
- 26) Uenishi T, Kubo S, Yamamoto T, Shuto T, Ogawa M, Tanaka H, et al. Cytokeratin 19 expression in hepatocellular carcinoma predicts early postoperative recurrence. *Cancer Sci* 2003;94:851-857.
- 27) Li W, Liang X, Kellendonk C, Poli V, Taub R. STAT3 contributes to the mitogenic response of hepatocytes during liver regeneration. *J Biol Chem* 2002;277:28411-28417.
- 28) Haga S, Ogawa W, Inoue H, Terui K, Ogino T, Igarashi R, et al. Compensatory recovery of liver mass by Akt-mediated hepatocellular hypertrophy in liver-specific STAT3-deficient mice. *J Hepatol* 2005;43:799-807.
- 29) Haga S, Ozaki M, Inoue H, Okamoto Y, Ogawa W, Takeda K, et al. The survival pathways phosphatidylinositol-3 kinase (PI3-K)/phosphoinositide-dependent protein kinase 1 (PDK1)/Akt modulate liver regeneration through hepatocyte size rather than proliferation. *HEPATOLOGY* 2009;49:204-214.
- 30) Gerlyng P, Abyholm A, Grotmol T, Erikstein B, Huitfeldt HS, Stokke T, et al. Binucleation and polyploidization patterns in developmental and regenerative rat liver growth. *Cell Prolif* 1993;26:557-565.
- 31) Miyaoka Y, Ebato K, Kato H, Arakawa S, Shimizu S, Miyajima A. Hypertrophy and unconventional cell division of hepatocytes underlie liver regeneration. *Curr Biol* 2012;22:1166-1175.
- 32) Hsu SH, Delgado ER, Otero PA, Teng KY, Kutay H, Meehan KM, et al. MicroRNA-122 regulates polyploidization in the murine liver. *HEPATOLOGY* 2016;64:599-615.
- 33) Aguilera A, Garcia-Muse T. Causes of genome instability. *Annu Rev Genet* 2013;47:1-32.
- 34) Terradas M, Martín M, Tusell L, Genescà A. DNA lesions sequestered in micronuclei induce a local defective-damage response. *DNA Repair* 2009;8:1225-1234.
- 35) Fenech M, Kirsch-Volders M, Natarajan AT, Surrallés J, Crott JW, Parry J, et al. Molecular mechanisms of micronucleus, nucleoplasmic bridge and nuclear bud formation in mammalian and human cells. *Mutagenesis* 2011;26:125-132.
- 36) Gisselsson D, Björk J, Höglund M, Mertens F, Cin PD, Akerman M, et al. Abnormal nuclear shape in solid tumors reflects mitotic instability. *Am J Pathol* 2001;158:199-206.
- 37) **Kang SH, Kwon JY, Lee JK, Seo YR.** Recent advances in *in vivo* genotoxicity testing: prediction of carcinogenic potential using comet and micronucleus assay in animal models. *J Cancer Prev* 2013;18:277-288.
- 38) Crasta K, Ganem NJ, Dagher R, Lantermann AB, Ivanova EV, Pan Y, et al. DNA breaks and chromosome pulverization from errors in mitosis. *Nature* 2012;482:53-58.
- 39) Cllet I, Fournier E, Melcion C, Cordier A. *In vivo* micronucleus test using mouse hepatocytes. *Mutat Res* 1989;216:321-326.
- 40) Igarashi M, Setoguchi M, Takada S, Itoh S, Furuhashi K. Optimum conditions for detecting hepatic micronuclei caused by numerical chromosome aberration inducers in mice. *Mutat Res* 2007;632:89-98.
- 41) Mullany LK, Nelsen CJ, Hanse EA, Goggin MM, Anttila CK, Peterson M, et al. Akt-mediated liver growth promotes induction of cyclin E through a novel translational mechanism and a p21-mediated cell cycle arrest. *J Biol Chem* 2007;282:21244-21252.
- 42) Yu H, Pardoll D, Jove R. STATs in cancer inflammation and immunity: a leading role for STAT3. *Nat Rev Cancer* 2009;9:798-809.
- 43) Wang Q, Yu WN, Chen X, Peng XD, Jeon SM, Birnbaum MJ, et al. Spontaneous hepatocellular carcinoma after the combined deletion of Akt isoforms. *Cancer Cell* 2016;29:523-535.
- 44) Guido M, Fassan M, Giacomelli L, Cillo U, Farinati F, Burra P, et al. Micronuclei and broken eggs in human liver carcinogenesis. *Anticancer Res* 2008;28:2507-2511.
- 45) Stephens PJ, Greenman CD, Fu B, Yang F, Bignell GR, Mudie LJ, et al. Massive genomic rearrangement acquired in a single catastrophic event during cancer development. *Cell* 2011;144:27-40.
- 46) **Zhang CZ, Spektor A, Cornils H, Francis JM, Jackson EK, Liu S, et al.** Chromothripsis from DNA damage in micronuclei. *Nature* 2015;522:179-184.
- 47) Naugler WE, Sakurai T, Kim S, Maeda S, Kim K, Elsharkawy AM, et al. Gender disparity in liver cancer due to sex differences in MyD88-dependent IL-6 production. *Science* 2007;317:121-124.
- 48) Park EJ, Lee JH, Yu GY, He G, Ali SR, Holzer RG, et al. Dietary and genetic obesity promote liver inflammation and tumorigenesis by enhancing IL-6 and TNF expression. *Cell* 2010;140:197-208.
- 49) Hunter CA, Jones SA. IL-6 as a keystone cytokine in health and disease. *Nat Immunol* 2015;16:448-457.

Author names in bold designate shared co-first authorship.

## Supporting Information

Additional Supporting Information may be found at [onlinelibrary.wiley.com/doi/10.1002/hep.29004/supinfo](http://onlinelibrary.wiley.com/doi/10.1002/hep.29004/supinfo).